Nanoparticles

DOI: 10.1002/anie.201003846

Programmed Nanoparticle Aggregation Using Molecular Beacons**

*Jonathan F. Lovell, Honglin Jin, Kenneth K. Ng, and Gang Zheng**

Nucleic acids can be used as robust building blocks or scaffolds for new nanoarchitectures.[1] The potential of nucleic acids has been demonstrated with the DNA-based construction of a variety of shapes including, for example, an incredible range of two-dimensional patterns,[2] three-dimensional crystals,[3] and even containers with lids that can be opened.[4] DNA scaffolds can be additionally functionalized with proteins to control enzyme cascades.[5] Nucleic acids play a prominent role in integrated nanoparticle–biomolecule hybrid systems and can induce the assembly of other nanoparticles, such as colloidal gold, into large macroscopic and even crystalline materials.[6–9] Other studies have demonstrated that gold nanoparticles themselves can induce the aggregation of proteins in solution.[10] Alternatively, surface-enhanced Raman scattering active nanoparticles can be used to detect protein aggregation.[11] Herein we describe a different type of aggregation phenomenon that is based on lipid nanoparticles, rather than metallic ones, and intraparticle forces generated by molecular beacons (MBs), rather than linker-based hybridization of nanoparticle networks. Irreversible aggregation of nanoparticles resulted from the opening of MBs inserted into nanoparticles.

We synthesized a MB functionalized with pyropheophorbide (Pyro) along with zero, one, two, or three BlackBerry quencher (BBQ) moieties as previously described.[12] The MB comprised a six-base stem and a 19-base loop (Figure 1a). The 5′ stem of the MB was also complementary to the target sequence since such shared-stem MBs have favorable thermodynamic profiles.[13] Both Pyro and BBQ are hydrophobic, and each additional quenching moiety additionally enhanced the MB hydrophobicity. We hypothesized that these increasingly hydrophobic MBs might insert into lipid nanoparticles such as low-density lipoprotein (LDL). As endogenous nanocarriers, lipoprotein nanoparticles are promising platforms for the delivery of contrast agents and drugs because of their small size, biocompatibility, and capacity to carry a range of cargo and even other small nanoparticles.[14–15] The LDL nanoparticle concentration was determined by examining the ApoB protein content, as each LDL is stabilized by only one ApoB protein. As shown in Figure 1b, upon incubation of the hydrophobically modified MBs with purified human LDL, hybrid nucleo-lipoprotein nanoparticles were generated and could be assessed using a gel-shift assay. Schematic representations of MB insertion into LDL are shown in Figure 1c. After the negatively charged beacons were inserted into the LDL, the electrophoretic mobility changed. When the beacon lacking any quenchers (0Q MB) was incubated with increasing amounts of LDL, it did not insert effectively into the nanoparticle (Figure 1b). A similar pattern was observed for the single-quencher MB (1Q MB) although at the 7.5:1 beacon/nanoparticle incubation ratio, approximately half the total amount of beacons inserted stably into the nanoparticles. When the 2Q MB was used, the majority of the beacon inserted into the LDL at the 15:1 beacon/nanoparticle

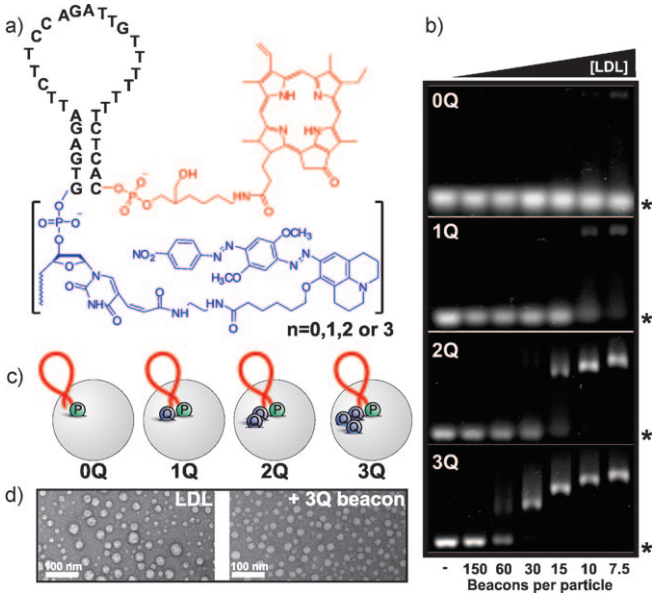

Figure 1. MB insertion into nanoparticles. a) Structure of MB modified with Pyro (red) and multiple BlackBerry quencher (BBQ) units (blue). b) Gel-shift assay demonstrating that multiple BBQ units enhance MB insertion into nanoparticles. 15 pmol of MB with the indicated number of BBQ units was incubated with increasing amounts of LDL, and then subjected to agarose gel electrophoresis. Asterisks indicate the migration of the unbound beacon while shifted bands correspond to nanoparticles containing the inserted beacon. c) Schematic illustration of the four different types of MBs with Pyro (P) and BBQ (Q) inserted into the LDL nanoparticles. d) Transmission electron micrographs of negative-stained LDL and LDL with the three-quencher beacon inserted.

[*] J. F. Lovell, K. K. Ng, Prof. G. Zheng
Institute of Biomaterials and Biomedical Engineering
University of Toronto (Canada)
H. Jin, Prof. G. Zheng
Department of Medical Biophysics, Ontario Cancer Institute
University of Toronto, Toronto, ON, M5G 1L7 (Canada)
E-mail: gang.zheng@uhnres.utoronto.ca
Homepage: http://www.utoronto.ca/zhenglab
H. Jin
Britton Chance Center for Biomedical Photonics
Huazhong University of Science and Technology
Wuhan (China)

[**] This work was supported by the Canadian Cancer Society, the Canadian Institute of Health Research, the Natural Sciences and Engineering Research Council of Canada, and the Joey and Toby Tanenbaum/Brazilian Ball Chair in Prostate Cancer Research.

Supporting information for this article is available on the WWW under http://dx.doi.org/10.1002/anie.201003846.

incubation ratio. Finally, when the 3Q MB was used, up to 30 beacons could be inserted into each LDL nanoparticle. Thus, the 3Q MB could most effectively insert into the lipid nanoparticles. To ensure beacons were completely inserted into the nanoparticles without requiring additional purification, the 3Q MB was used in subsequent experiments with a low beacon/nanoparticle ratio of six beacons per nanoparticle. MBs did not drastically alter the size and shape of the LDL nanoparticle, as revealed by transmission electron microscopy when comparing unmodified LDL to LDL having the inserted 3Q MBs (Figure 1 d).

When the target nucleic acid was added to the nanoparticles in which 3Q MB was inserted, unexpected and visible aggregation occurred (Figure 2 a). The aggregates were pelleted by centrifugation, and were then assessed for

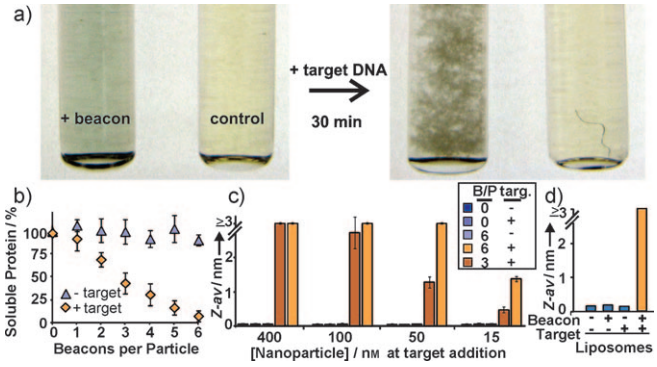

Figure 2. Nanoparticle aggregation induced by target DNA. a) Photographs of visible aggregation induced by target DNA. LDL was incubated with or without six MBs per particle. A tenfold molar excess of target DNA was added and incubated for 30 min. A piece of dust is seen in the control tube after target addition. b) Protein aggregation of LDL nanoparticles as a function of the number of MBs per nanoparticle. Error bars show the standard deviation (n = sample size of 3). c) Dynamic light scattering shows that aggregation is modulated by both the nanoparticle concentration and the number of beacons per particle (B/P). Large Z averages indicate aggregation (instrument detection limit was 3 microns). Error bars show the standard deviation (n = sample size of 3). d) Aggregation of liposomes detected by dynamic light scattering. Liposomes (6:4 DSPC/choleterol) were incubated with 3Q MB and target as indicated.

ApoB content. The insoluble aggregates included the ApoB protein, and a concentration-dependent aggregation pattern was observed in which full nanoparticle precipitation could be achieved with six beacons inserted per particle (Figure 2 b). We next made use of dynamic light scattering to assess aggregation of the nanoparticles (Figure 2 c). The upper detection limit for the light-scattering instrumentation was 3 microns, whereas standard LDL is approximately 25 nm in diameter. A limitation of this assay was that when there was a small amount of aggregation, light scattering could not accurately distinguish between a small population of large aggregates or a homogeneous population of smaller aggregates. Therefore, this assay was used to verify the aggregation state, and not for insight into the shape and size distributions of the aggregates. At nanoparticle concentrations of 400 nM and 100 nM, aggregation was observed with target addition to nanoparticles bearing three or six beacons per particle. At 50 nM nanoparticle concentration, only the nanoparticle with six beacons per nanoparticle displayed full aggregation, and the nanoparticle with three MBs per nanoparticle exhibited less aggregation. At 15 nM nanoparticle concentration, nanoparticles with six beacons per nanoparticle displayed diminished aggregation, and those with three beacons per nanoparticle had minimal aggregation compared to those at the 50 nM nanoparticle concentration. Therefore, the nanoparticle aggregation process was modulated both by the number of MBs per nanoparticle and the nanoparticle concentration at target addition. Since the aggregates contained the ApoB protein (Figure 2 b), we next examined whether or not a proteinacious component was essential for the aggregation phenomena. When distearoylphosphatidylcholine (DSPC)/cholesterol (6:4) liposomes were incubated with the 3Q MB, only a small fraction of beacon binding was observed (data not shown). Despite the incomplete beacon binding, addition of the target nucleic acid to the liposomes incubated with the beacon specifically induced aggregation (Figure 1 d). Therefore, neither protein aggregation nor a protein component was essential for nanoparticle aggregation, suggesting that aggregation is based on the interactions between lipids and structural rearrangements resulting from the hydrophobically modified MBs upon opening.

We next examined whether the MB-driven aggregation could recognize single-base mismatches (Figure 3 a). When a 16-base target was used, aggregation occurred even when a mismatch was introduced. When a 15 mer target was used, aggregation was less efficient for the single-base mismatch target. When 14 mer and 13 mer targets were used, aggregation was observed for only the correct target sequence. When

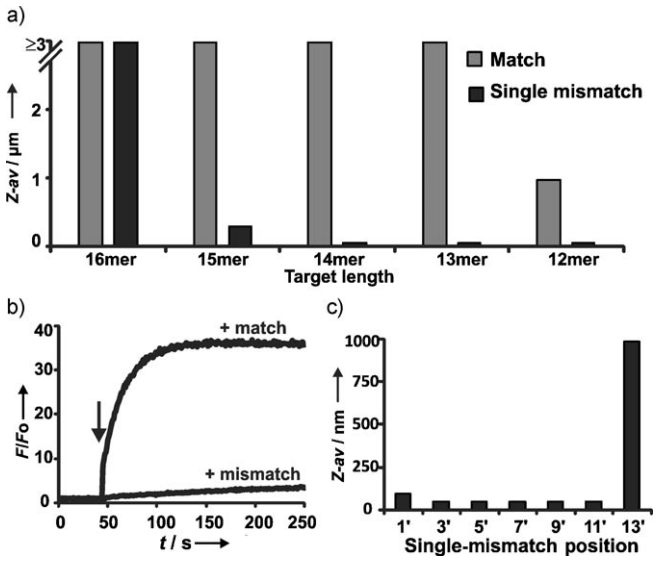

Figure 3. Single-base mismatch discrimination. a) Aggregation induced by targets of various lengths with or without a single-base mismatch. b) Fluorescence response upon addition of the 13 mer target with or without a single-base mismatch. At the indicated time, target was added and fluorescence was monitored. F corresponds to the fluorescence and F_o is the initial fluorescence of the beacon. c) Effect of mismatch position on aggregation using a 13 mer target containing a single mismatch.

the target length was reduced to a 12 mer, even the correct target sequence induced diminished aggregation. These results were consistent with a process dependent upon opening of the MB. This was additionally supported by the observation that the 13 mer single-base-mismatch target could not effectively open the MB, but the matched 13 mer target could, leading to fluorescence (Figure 3 b). The location of the mismatch within the target sequence was also considered by examining single-base mismatches at every other position in the 13 mer target. Since the target was a shared-stem target, the last six bases of the target hybridized with the 5′ MB stem, and the first eight bases of the target hybridized to the loop portion of the MB. With one exception, single-base-mismatch targets could not induce aggregation, regardless of the mismatch position. When the 13′ position was mismatched, partial aggregation was observed. This base hybridized with the very first base of 5′ beacon terminal, suggesting that this position is important for the aggregation.

In summary, MBs inserted into lipoprotein and liposome lipid nanoparticles and selectively induced irreversible nanoparticle aggregation through target nucleic acid recognition. In the presence of the target, the process was modulated by two controllable variables: nanoparticle concentration and the number of beacons per particle. This phenomenon is a promising new technique for DNA–nanoparticle manipulations. Future work will examine beacon and target sequences having varying lengths and G-C content, and will explore directed aggregation using payload-bearing nanoparticles on surfaces decorated with target DNA.

Received: June 23, 2010
Published online: September 17, 2010

Keywords: aggregation · DNA · lipoproteins · molecular beacons · nanoparticles

[1] U. Feldkamp, C. M. Niemeyer, *Angew. Chem.* **2006**, *118*, 1888 – 1910; *Angew. Chem. Int. Ed.* **2006**, *45*, 1856 – 1876.
[2] P. W. K. Rothemund, *Nature* **2006**, *440*, 297 – 302.
[3] J. Zheng, J. J. Birktoft, Y. Chen, T. Wang, R. Sha, P. E. Constantinou, S. L. Ginell, C. Mao, N. C. Seeman, *Nature* **2009**, *461*, 74 – 77.
[4] E. S. Andersen, M. Dong, M. M. Nielsen, K. Jahn, R. Subramani, W. Mamdouh, M. M. Golas, B. Sander, H. Stark, C. L. P. Oliveira, et al., *Nature* **2009**, *459*, 73 – 76.
[5] O. I. Wilner, Y. Weizmann, R. Gill, O. Lioubashevski, R. Freeman, I. Willner, *Nat. Nanotechnol.* **2009**, *4*, 249 – 254.
[6] D. Nykypanchuk, M. M. Maye, D. van der Lelie, O. Gang, *Nature* **2008**, *451*, 549 – 552.
[7] C. A. Mirkin, R. L. Letsinger, R. C. Mucic, J. J. Storhoff, *Nature* **1996**, *382*, 607 – 609.
[8] E. Katz, I. Willner, *Angew. Chem.* **2004**, *116*, 6166 – 6235; *Angew. Chem. Int. Ed.* **2004**, *43*, 6042 – 6108.
[9] S. Y. Park, A. K. R. Lytton-Jean, B. Lee, S. Weigand, G. C. Schatz, C. A. Mirkin, *Nature* **2008**, *451*, 553 – 556.
[10] D. Zhang, O. Neumann, H. Wang, V. M. Yuwono, A. Barhoumi, M. Perham, J. D. Hartgerink, P. Wittung-Stafshede, N. J. Halas, *Nano Lett.* **2009**, *9*, 666 – 671.
[11] D. C. Kennedy, L. Tay, R. K. Lyn, Y. Rouleau, J. Hulse, J. P. Pezacki, *ACS Nano* **2009**, *3*, 2329 – 2339.
[12] J. F. Lovell, J. Chen, E. Huynh, M. T. Jarvi, B. C. Wilson, G. Zheng, *Bioconjugate Chem.* **2010**, *21*, 1023 – 1025.
[13] A. Tsourkas, M. A. Behlke, G. Bao, *Nucleic Acids Res.* **2002**, *30*, 4208 – 4215.
[14] D. P. Cormode, T. Skajaa, M. M. van Schooneveld, R. Koole, P. Jarzyna, M. E. Lobatto, C. Calcagno, A. Barazza, R. E. Gordon, P. Zanzonico, et al., *Nano Lett.* **2008**, *8*, 3715 – 3723.
[15] G. Zheng, J. Chen, H. Li, J. D. Glickson, *Proc. Natl. Acad. Sci. USA* **2005**, *102*, 17757 – 17762.

